Molecular Crystals and Liquid Crystals

ISSN: 1542-1406 (Print) 1563-5287 (Online) Journal homepage: http://www.tandfonline.com/loi/gmcl20

Synthesis, structure, and mesomorphism of novel liquid crystalline acrylate monomers and polymers

Xiao-Xu Xu, Chun-Ying Chao & Xi-Jing Yao

To cite this article: Xiao-Xu Xu, Chun-Ying Chao & Xi-Jing Yao (2016) Synthesis, structure, and mesomorphism of novel liquid crystalline acrylate monomers and polymers, Molecular Crystals and Liquid Crystals, 624:1, 1-10, DOI: 10.1080/15421406.2015.1017295

To link to this article: http://dx.doi.org/10.1080/15421406.2015.1017295

Published online: 11 Feb 2016.

MOL. CRYST. LIQ. CRYST.
2016, VOL. 624, NO. 1, 1–10
http://dx.doi.org/10.1080/15421406.2015.1017295

Taylor & Francis
Taylor & Francis Group

Synthesis, structure, and mesomorphism of novel liquid crystalline acrylate monomers and polymers

Xiao-Xu Xu[a], Chun-Ying Chao[b], and Xi-Jing Yao[b]

[a]College of Chemical Engineering and Material, Eastern Liaoning University, Dandong, P. R. China; [b]Center for Molecular Science and Engineering, College of Science, Northeastern University, Shenyang, P. R. China

ABSTRACT

A series of novel liquid crystalline monomers ($\mathbf{M_1}$—$\mathbf{M_8}$) and side chain polymers base polyacrylate backbone were synthesized. The chemical structures were characterized by FT-IR and ^{1}H-NMR spectra. The mesomorphism and thermal behavior was investigated by polarizing optical microscopy, differential scanning calorimetry, and thermogravimetric analysis. The relationships of structure and mesomorphism are discussed in detail. The eight monomers and their corresponding polymers all show enantiotropic nematic phase. With increasing the spacer length or flexibility of the terminal group, the melting temperature (T_m) and isotropic temperature (T_i) of the corresponding monomers and polymers all decreased. However, with increasing the rigidity of the mesogenic core, T_m and T_i of the corresponding monomers and polymers all increased. TGA showed that all the polymers obtained in this study had excellent thermal stability.

KEYWORDS

Acrylate monomer; liquid crystalline polymer; nematic phase; synthesis

1. Introduction

The area of liquid crystals (LCs) arguably is one of the most extensive and dynamic fields of present-day materials research [1, 2]. LC materials combine order and mobility and form well-organized supramolecular assemblies that exhibit a variety of physical properties [3–6]. Therefore, as new functional materials, they can provide interesting studies of molecular aggregation in which the driving forces of self assembly can be studied in a systematic and controlled manner [7].

For side chain liquid crystalline polymers (LCPs), their mesomorphism depends on the nature of polymer backbone, the type of mesogen, the flexible spacer length, and the nature of terminal groups [8–15]. The mesogens are usually attached to the polymer backbone through the flexible spacer. The polymer backbone and mesogens have antagonistic tendencies: the polymer backbone is driven toward a random coil-type configuration, whereas the mesogens stabilize with long-range orientational order. The flexible spacer, which is usually an aliphatic hydrocarbon chain containing, normally, more than two methylene units, decouples the mesogenic side groups from the polymer backbone and renders the mesogens to orientational order. Recently, many new LC materials have been reported [16–22]. Therefore, it is

CONTACT Xiao-Xu Xu 3x.931@163.com College of Chemical Engineering and Material, Eastern Liaoning University, Dandong, 118004, P. R. China.
Color versions of one or more of the figures in the article can be found online at www.tandfonline.com/gmcl.

both necessary and useful to synthesize various kinds of LC material to study the relationship of the structure and properties, and explore their potential applications.

In this paper, eight new LC monomers and polymers were prepared and characterized. The mesomorphism and thermal behavior were investigated with polarizing optical microscopy (POM), differential scanning calorimetry (DSC) and thermogravimetric analysis (TGA). The structure–property relationships of the monomers and polymers obtained in this study are discussed.

2. Experimental

2.1. *Materials*

2-Chloroethanol was purchased from Tianjin Dagu Chemical Plant. 6-Chlorohexanol from Zhouping Mingxing Chemical Engineering Co., Ltd. 4-Hydroxybenzoic acid was obtained from Shanghai Wulian Chemical Plant. Acrylic acid was purchased from Shenyang Hefu Chemical Reagent Co., Ltd. 4-Ethylbenzoic acid and *p*-benzenediol was purchased from Beijing Chemical Plant. 4-Pentylbenzoic acid was purchased from Yantai Xianhua Chemical Engineering Co., Ltd. 4,4′-Dihydroxybiphenyl (from Aldrich) was used as received. All solvents and reagents used were purified by standard methods.

2.2. *Measurements*

FT-IR spectra were measured on a Perkin-Elmer spectrum One (B) spectrometer. ^{1}H-NMR spectra were obtained with a Bruker ARX400 spectrometer. The average molecular weight of the polymer was obtained with Waters gel permeation chromatography (GPC) 1515. A Leica DMRX POM equipped with a Linkam THMSE-600 heating and cooling stage was used to observe the phase transition temperatures and analyze the mesomorphism through the observation of optical textures. The phase behavior was determined with a Netzsch DSC 204 equipped with a cooling system. The heating and cooling rates were 10°C/min. Thermal decomposition temperature data were measured under nitrogen atmosphere with a Netzsch TGA 209C thermogravimetric analyzer at a heating rate of 20°C/min.

2.3. *Synthesis of the compounds*

The synthetic route of the compounds **1**–**8** is outlined in Scheme 1. 4-(2-Hydroxyethoxy)benzoic acid (**1**), 4-(6-hydroxyhexyloxy)benzoic acid (**2**),

4-(2-(acryloyloxy)ethoxy)benzoic acid (**3**), and 4-(6-(acryloyloxy)hexyloxy) benzoic acid (**4**) were prepared according to the method reported previously [23–25].

2.3.1. *4-Hydroxyphenyl-4′-ethylbenzoate (5)*

4-Ethylbenzoyl chloride (16.8 g, 0.1 mol) was dissolved in 20 mL of dry tetrahydrofuran (THF), and then added dropwise to the stirred solution of *p*-benzenediol (55 g, 0.5 mol) in 200 mL of THF and 8mL of pyridine. The mixture was reacted for 4 hr at room temperature, and refluxed for 6 hr. After the reaction solution was concentrated, the residue was poured into beaker filled with 500 mL of ice-water, the crude product was washed with warm water, and recrystallized from ethanol. Yield: 67 %. mp: 132°C. FT-IR (KBr, cm^{-1}): 3447 (–OH); 2971, 2880 (CH_3–, –CH_2–); 1713 (C=O); 1605, 1575 (Ar–).

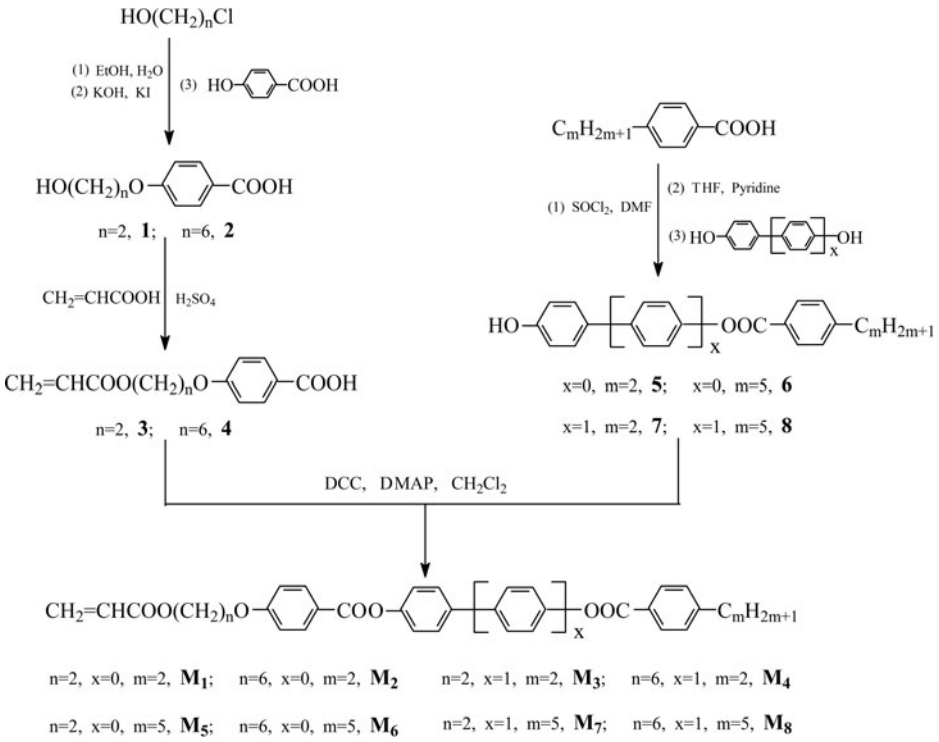

Scheme 1. Synthesis of the compounds **1**–**8** and monomers $\mathbf{M_1}$—$\mathbf{M_8}$.

2.3.2. *4-Hydroxyphenyl-4′-pentylbenzoate (6)*

The compound **6** was prepared by a procedure similar to that for **5**. Recrystallized from ethanol. Yield: 63%. mp: 110°C. FT-IR (KBr, cm^{-1}): 3387 (–OH); 2952, 2826 (CH_3–, –CH_2–); 1721 (C=O); 1600, 1510 (Ar–).

2.3.3. *4-Hydroxybiphenyl-4′-ethylbenzoate (7)*

4-Pentylbenzoyl chloride (8.4 g, 0.04 mol) was dissolved in 10 mL of dry tetrahydrofuran (THF), and then added dropwise to the stirred solution of 4,4′-dihydroxybiphenyl (29.8 g, 0.16 mol) in 120 mL of THF and 4mL of pyridine. After the mixture was refluxed for 10h, the reaction solution was poured into beaker filled with 1000 mL of ice-water, the crude product, obtained by filtration, was washed with 1.5% NaOH solution and ethanol, and recrystallized from ethanol/acetone (1:1). Yield: 33%. mp: 211°C. FT-IR (KBr, cm^{-1}): 3390 (–OH); 2962, 2876 (CH_3–, –CH_2–); 1726 (C=O); 1606, 1583 (Ar–).

2.3.4. *4-Hydroxybiphenyl-4′-pentylbenzoate (8)*

The compound **8** was prepared by a procedure similar to that for **7**. Recrystallized from ethanol/acetone (2:1). Yield: 339%. mp: 173°C. FT-IR (KBr, cm^{-1}): 3420 (–OH); 2960, 2818 (CH_3–, –CH_2–); 1738 (C=O); 1613, 1594 (Ar–).

2.4. *Synthesis of the monomers*

The synthetic route of the acrylate monomers $\mathbf{M_1}$–$\mathbf{M_8}$ is shown in Scheme 1. The synthesis of $\mathbf{M_1}$–$\mathbf{M_8}$ is presented by the same method.

2.4.1. *4-(4-(2-(Acryloyloxy)ethoxy)benzoyloxy)phenyl-4′-ethylbenzoate (M_1)*

The compounds **3** (2.36 g, 0.01 mol) and **5** (2.42 g, 0.01 mol) were dissolved in 45 ml of CH_2Cl_2 at 30°C. *N*,*N*′-Dicyclohexylcarbodiimide (DCC) (1.03 g, 0.01 mol) and a small amount of 4-dimethylaminopyridine (DMAP) were dissolved in 5 ml of CH_2Cl_2, and then added dropwise to the above solution. The reaction mixture was stirred for 24 hr at 30°C. After a small amount of water was added into the resulting solution, and filtered. The filtrate was dried with anhydrous $MgSO_4$, and evaporated to dryness. The crude product obtained was purified by silica gel column chromatography (ethyl acetate/hexane = 1/2). White solid was obtained. Yield: 72%. FT-IR (KBr, cm^{-1}): 3028 (=C—H); 2967, 2872 (–CH_2–); 1731, 1714 (C=O); 1636 (C=C); 1605, 1575 (Ar–); 1277 (C—O—C). ^{1}H-NMR ($CDCl_3$, TMS, δ, ppm): 1.23–1.28 (t, 3H, –C***H***$_3$); 2.70–2.75 (m, 2H, –C***H***$_2$$CH_3$); 4.25–4.54 [m, 4H, –COO(C***H***$_2$)$_2$O–)]; 5.84–5.87 and 6.41–6.46 (m, 2H, C***H***$_2$ =); 6.12–6.19 (m, 1H, CH_2 = C***H***–); 6.97–8.16 (m, 12H, Ar—***H***).

2.4.2. *4-(4-(6-(Acryloyloxy)hexyloxy)benzoyloxy)phenyl-4′-ethylbenzoate (M_2)*

Purified by silica gel column chromatography (ethyl acetate/hexane = 1/2). White solid was obtained. Yield: 62%. FT-IR (KBr, cm^{-1}): 3075 (=C–H); 2958, 2854 (–CH_2–); 1744, 1727 (C=O); 1636 (C=C); 1601, 1579 (Ar–); 1268 (C–O–C). ^{1}H-NMR ($CDCl_3$, TMS, δ, ppm): 1.24–1.28 (t, 3H, –C***H***$_3$); 1.45–1.82 [m, 8H, –COOCH_2(C***H***$_2$)$_4$$CH_2$O–)]; 2.71–2.76 (m, 2H, –C***H***$_2$$CH_3$); 3.99 [t, 2H, –COOC***H***$_2$(CH_2)$_4$$CH_2$O–)]; 4.12 [t, 2H, –COOC$H_2$($CH_2$)$_4$C***H***$_2$O–)]; 5.85–5.87 and 6.41–6.47 (m, 2H, C***H***$_2$ =); 6.11–6.17 (m, 1H, CH_2 = C***H***–); 7.01–8.18 (m, 12H, Ar–***H***).

2.4.3. *4-(4-(2-(Acryloyloxy)ethoxy)benzoyloxy)biphenyl-4′-ethylbenzoate (M_3)*

Purified by silica gel column chromatography (ethyl acetate/hexane = 1/1). White solid was obtained. Yield: 52%. FT-IR (KBr, cm^{-1}): 3036 (=C–H); 2961, 2872 (–CH_2–); 1739, 1714 (C=O); 1636 (C=C); 1601, 1571 (Ar–); 1278 (C–O–C). ^{1}H-NMR ($CDCl_3$, TMS, δ, ppm): 1.23–1.29 (t, 3H, –C***H***$_3$); 2.71–2.75 (m, 2H, –C***H***$_2$$CH_3$); 4.27–4.55 [m, 4H, –COO(C***H***$_2$)$_2$O–)]; 5.85–5.89 and 6.40–6.46 (m, 2H, C***H***$_2$ =); 6.14–6.20 (m, 1H, CH_2 = C***H***–); 6.99–8.19 (m, 16H, Ar–***H***).

2.4.4. *4-(4-(6-(Acryloyloxy)hexyloxy)benzoyloxy)biphenyl-4′-ethylbenzoate (M_4)*

Purified by silica gel column chromatography (ethyl acetate/hexane = 1/1). White solid was obtained. Yield: 61%. FT-IR (KBr, cm^{-1}): 3062 (=C–H); 2932, 2859 (–CH_2–); 1735 (C=O); 1635 (C=C); 1601, 1571 (Ar–); 1272 (C–O–C). ^{1}H-NMR ($CDCl_3$, TMS, δ, ppm): 1.25–1.28 (t, 3H, –C***H***$_3$); 1.46–1.83 [m, 8H, –COOCH_2(C***H***$_2$)$_4$$CH_2$O–)]; 2.70–2.76 (m, 2H, –C***H***$_2$$CH_3$); 4.01 [t, 2H, –COOC***H***$_2$(CH_2)$_4$$CH_2$O–)]; 4.15 [t, 2H, –COOC$H_2$($CH_2$)$_4$C***H***$_2$O–)]; 5.85–5.88 and 6.43–6.48 (m, 2H, C***H***$_2$ =); 6.13–6.18 (m, 1H, CH_2 = C***H***–); 7.00–8.19 (m, 16H, Ar–***H***).

2.4.5. *4-(4-(2-(Acryloyloxy)ethoxy)benzoyloxy)phenyl-4′-pentylbenzoate (M_5)*

Purified by silica gel column chromatography (ethyl acetate/hexane = 1/2). White solid was obtained. Yield: 63%. FT-IR (KBr, cm^{-1}): 3035 (=C–H); 2953, 2828 (–CH_2–); 1735 (C=O); 1639 (C=C); 1605, 1583 (Ar–); 1254 (C–O–C). ^{1}H-NMR ($CDCl_3$, TMS, δ, ppm): 0.91–1.71 [m, 9H, –CH_2(CH_2)$_3$C***H***$_3$)]; 2.68–2.72 [t, 2H, –C***H***$_2$(CH_2)$_3$$CH_3$)]; 4.32–4.58 [m, 4H, –COO(C***H***$_2$)$_2$O–)]; 5.85–5.90 and 6.45–6.49 (m, 2H, C***H***$_2$ =); 6.17–6.21 (m, 1H, CH_2 = C***H***–); 7.02–8.18 (m, 12H, Ar–***H***).

2.4.6. *4-(4-(6-(Acryloyloxy)hexyloxy)benzoyloxy)phenyl-4′-pentylbenzoate (M_6)*

Purified by silica gel column chromatography (ethyl acetate/hexane = 1/2). White solid was obtained. Yield: 45%. FT-IR (KBr, cm^{-1}): 3031 (=C–H); 2932, 2858 (–CH_2–); 1732 (C=O); 1639 (C=C); 1606, 1580 (Ar–); 1273 (C–O–C). ^{1}H-NMR ($CDCl_3$, TMS, δ, ppm): 0.90–0.94 (m, 3H, –C***H***$_3$); 1.35–1.85 [m, 14H, –CH_2(C***H***$_2$)$_3$$CH_3$) and –$COOCH_2$(C***H***$_2$)$_4$$CH_2O$–)]; 2.69–2.72 [t, 2H, –C***H***$_2$(CH_2)$_3$$CH_3$)]; 4.02 [t, 2H, –$COOCH_2$(C***H***$_2$)$_4$$CH_2O$–)]; 4.17 [t, 2H, –$COOCH_2$($CH_2$)$_4$C***H***$_2$O–)]; 5.85–5.89 and 6.43–6.48 (m, 2H, C***H***$_2$ =); 6.15–6.20 (m, 1H, CH_2 = C***H***–); 7.01–8.18 (m, 12H, Ar–***H***).

2.4.7. *4-(4-(2-(Acryloyloxy)ethoxy)benzoyloxy)biphenyl-4′-pentylbenzoate (M_7)*

Purified by silica gel column chromatography (ethyl acetate/hexane = 1/1). White solid was obtained. Yield: 57%. FT-IR (KBr, cm^{-1}): 3071 (=C–H); 2955, 2854 (–CH_2–); 1732, 1723 (C=O); 1640 (C=C); 1601, 1571 (Ar–); 1276 (C–O–C). ^{1}H-NMR ($CDCl_3$, TMS, δ, ppm): 0.90–1.71 [m, 9H, –CH_2(C***H***$_2$)$_3$C***H***$_3$)]; 2.70–2.73 [t, 2H, –C***H***$_2$(CH_2)$_3$$CH_3$)]; 4.33–4.58 [m, 4H, –COO(C***H***$_2$)$_2$O–)]; 5.84–5.90 and 6.46–6.51 (m, 2H, C***H***$_2$ =); 6.17–6.22 (m, 1H, CH_2 = C***H***–); 7.02–8.20 (m, 16H, Ar–***H***).

2.4.8. *4-(4-(6-(Acryloyloxy)hexyloxy)benzoyloxy)biphenyl-4′-pentylbenzoate (M_8)*

Purified by silica gel column chromatography (ethyl acetate/hexane = 1/2). White solid was obtained. Yield: 63%. FT-IR (KBr, cm^{-1}): 3056 (=C–H); 2956, 2829 (–CH_2–); 1732 (C=O); 1636 (C=C); 1604, 1578 (Ar–); 1276 (C–O–C). ^{1}H-NMR ($CDCl_3$, TMS, δ, ppm): 0.91–0.93 (m, 3H, –C***H***$_3$); 1.34–1.86 [m, 14H, –CH_2(C***H***$_2$)$_3$$CH_3$) and –$COOCH_2$(C***H***$_2$)$_4$$CH_2O$–)]; 2.70–2.73 [t, 2H, –C***H***$_2$(CH_2)$_3$$CH_3$)]; 4.05 [t, 2H, –COOC***H***$_2$(CH_2)$_4$$CH_2O$–)]; 4.18 [t, 2H, –$COOCH_2$($CH_2$)$_4$C***H***$_2$O–)]; 5.84–5.89 and 6.42–6.47 (m, 2H, C***H***$_2$ =); 6.16–6.20 (m, 1H, CH_2 = C***H***–); 7.03–8.21 (m, 16H, Ar–***H***).

2.5. *Synthesis of the polymers*

The synthetic route of the polymers $\mathbf{P_1}$—$\mathbf{P_8}$ is shown in Scheme 2. The yields and average molecular weight of $\mathbf{P_1}$—$\mathbf{P_8}$ are summarized in Table 1. The eight polymers were prepared by the radical polymerization of monomers in a sealed ampoule tube with anhydrous toluene using azobisisobutyronitrile (AIBN, 3 mol% to the monomer) as an initiator at 60°C for 24 hr under nitrogen conditions. The crude polymers were precipitated in a large amount of methanol solution, and then purified by dissolving them in toluene and reprecipitated in methanol, and then dried in a vacuum.

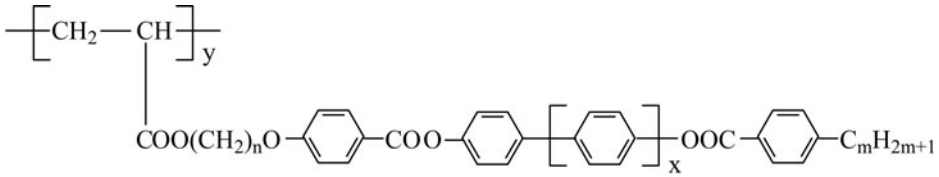

n=2, x=0, m=2, $\mathbf{P_1}$; n=6, x=0, m=2, $\mathbf{P_2}$ n=2, x=1, m=2, $\mathbf{P_3}$; n=6, x=1, m=2, $\mathbf{P_4}$

n=2, x=0, m=5, $\mathbf{P_5}$; n=6, x=0, m=5, $\mathbf{P_6}$ n=2, x=1, m=5, $\mathbf{P_7}$; n=6, x=1, m=5, $\mathbf{P_8}$

Scheme 2. Synthesis of the polymers $\mathbf{P_1}$—$\mathbf{P_8}$.

Table 1. Yields and average molecular weights of polymers.

Polymer	Yield/ %	M_n($\times 10^4$ g/mol)	M_w($\times 10^4$ g/mol)	PDI
P_1	89	1.63	2.06	1.26
P_2	90	1.78	2.47	1.39
P_3	91	1.56	2.19	1.40
P_4	92	1.65	2.38	1.44
P_5	90	1.69	2.27	1.34
P_6	88	1.83	2.42	1.32
P_7	87	1.71	2.35	1.37
P_8	89	1.62	2.29	1.41

[a]Data determined by GPC in THF using PS standards.
[b]PDI = M_w/ M_n, dispersion coefficient.

3. Results and discussion

3.1. *Mesomorphism of the monomers*

The mesomorphism of the monomers was characterized with POM and DSC. POM results showed that **M$_1$**−**M$_8$** exhibited enantiotropic nematic a thread-like Schlieren texture on heating and cooling cycles. As an example, the optical textures of **M$_1$** are shown in Fig. 1. Table 2 summarizes the phase transition temperatures, enthalpy changes and mesophase types of **M$_1$**−**M$_8$**. On heating cycle, eight monomers all showed a melting transition at low temperature, only **M$_1$**, **M$_2$**, **M$_4$**, **M$_5$**, and **M$_6$** revealed an obvious nematic to isotropic phase transition at high temperature. On cooling cycle, an isotropic to nematic phase transition except for **M$_3$**, **M$_7$**, and **M$_8$**, and a crystallization transition for all the monomers appeared. However, POM results confirmed that **M$_3$**, **M$_7$**, and **M$_8$** exhibited excellent mesomorphism and typical nematic texture. Therefore, the isotropic temperatures (T_i) of **M$_3$**, **M$_7$**, and **M$_8$**, listed in Table 2, were obtained with POM. According to Table 2, the molecular structure had a considerable influence on the thermal behavior of **M$_1$**−**M$_8$**. The effect of the spacer length, mesogenic core rigidity, and terminal group on the melting temperature (T_m) and T_i was discussed in detail as follows.

3.1.1. *The effect of the spacer length*

In general, with increasing the spacer length, the intermolecular forces weaken, which make the thermal behavior change, and the phase transition temperatures decrease. For example, **M$_1$** and **M$_2$** had same mesogenic core and terminal groups, but the spacer length was different. Compared with **M$_1$** containing two methylene spacers, T_m and T_i of **M$_2$** containing six methylene spacer decreased by 37.3 and 1.3°C, respectively. Similarly, T_m and T_i of **M$_4$** decreased by 54.5 and 3.7°C than those of **M$_3$**; T_m and T_i of **M$_6$** decreased by 55.9 and 9.9°C than those of **M$_5$**; T_m and T_i of **M$_8$** decreased by 36.1 and 15.0°C than those of **M$_7$**. According to the above data, with increasing the spacer length, the corresponding T_m and T_i all decreased, moreover, the T_m decreased more than T_i, so the mesophase temperature range widened.

3.1.2. *The effect of the mesogenic core rigidity*

With increasing the rigidity of the mesogenic core or the number of aryl rings in LC molecules, the corresponding T_m and T_i increased. Taking the effect of the number of aryl rings on T_i into account, the equation is given by Dejeu [26] as follows:

$$T_i = \frac{0.084(\alpha_{//} - \alpha_{\perp})I}{KV^2} \quad (1)$$

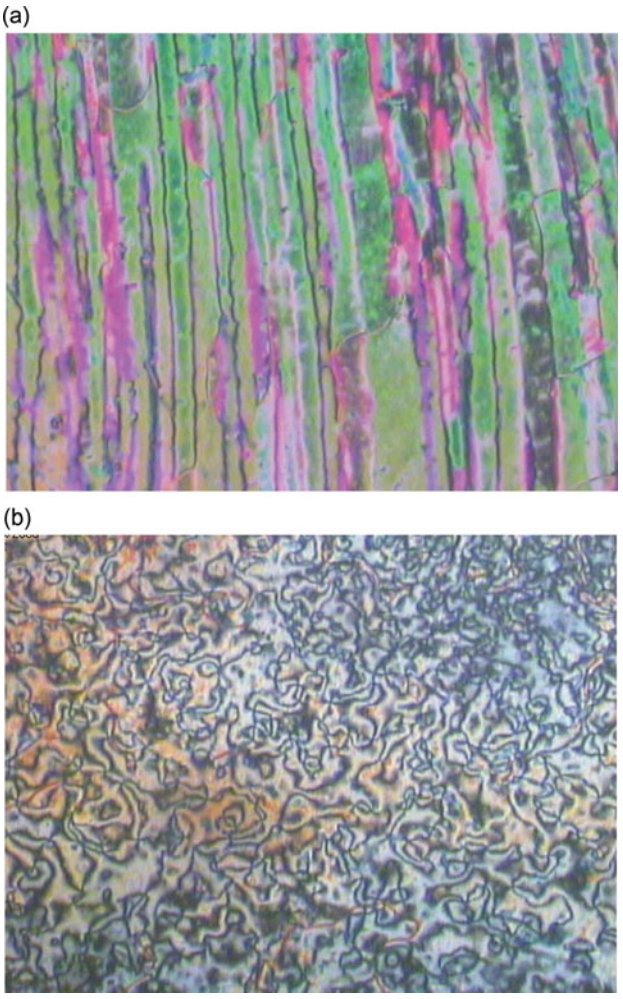

Figure 1. Optical textures of $\mathbf{M_1}$ (200×). (a) thread-like texture of nematic phase; (b) Schlieren texture of nematic phase.

Where K is Boltzman's constant, I is ionized electric potential, V is molar volume, and $\alpha_{//} - \alpha_{\perp}$ is polarizability anisotropy parallel and normal to molecular axis direction. In the conjugate system of the aryl rings, the $\alpha_{//}$-value is very great, so the $\alpha_{//}$-value will increase with increasing the number of the aryl rings, and T_i also increases. For example, $\mathbf{M_1}$ and $\mathbf{M_3}$ had same spacer length and terminal groups, but the mesogenic core was different. Compared

Table 2. Phase transition temperature (°C) and enthalpy changes ($J \cdot g^{-1}$) of the monomers.

Monomer	Mesophase and phase transitions/ Heating/Cooling	
M_1	Cr149.5(91.4)N171.1(0.6)I	I169.1(0.1)N73.6(57.4)Cr
M_2	Cr112.2(60.6)N169.8(0.3)I	I168.4(0.2)N55.2(33.7)Cr
M_3	Cr183.3(76.6)N332.5[a]I	328.6[a]N175.3(26.2)Cr
M_4	Cr128.8(45.1)N328.8(1.1)I	I320.5(1.6)N90.4(4.6)Cr
M_5	Cr127.2(78.3)N162.8(1.0)I	I160.1(0.1)N66.5(31.6)Cr
M_6	Cr71.3(65.8)N152.9(1.2)I	I149.6(0.2)N57.1(11.8)Cr
M_7	Cr153.7(30.6)N326.7[a]I	I307.8[a]N147.8(10.5)Cr
M_8	Cr117.6(21.2)N311.7[a]I	I301.3[a]N110.7(10.1)Cr

Cr = crystal, N = nematic; I = isotropic.
[a]Data obtained by POM.

with **M$_1$** containing three phenyl rings in the mesogenic core, T_m and T_i of **M$_3$** containing four phenyl rings increased by 33.8 and 161.4°C, respectively. Similarly, T_m and T_i of **M$_4$** increased by 16.6 and 159.0°C than those of **M$_2$**; T_m and T_i of **M$_7$** increased by 26.5 and 163.9°C than those of **M$_5$**; T_m and T_i of **M$_8$** increased by 46.3 and 158.8°C than those of **M$_6$**. According to the above data, T_i increased more than T_m with an increase of phenyl rings, so the mesophase temperature ranges widened.

3.1.3. *The effect of the terminal group*

The flexibility and polarity of the terminal group also can affect the phase transition temperatures. With increasing the flexibility *a* of the terminal group, the corresponding T_m and T_i decreased, which also is similar to the effect of the spacer length. For example, **M$_1$** and **M$_5$** had same spacer length and mesogenic core, but the terminal group was different. Compared with **M$_1$** containing terminal ethyl group, T_m and T_i of **M$_5$** containing terminal pentyl group decreased by 22.3 and 8.3°C, respectively. Similarly, T_m and T_i of **M$_6$** decreased by 40.9 and 16.9°C than those of **M$_2$**; T_m and T_i of **M$_7$** decreased by 29.6 and 5.8°C than those of **M$_3$**; T_m and T_i of **M$_8$** decreased by 11.2 and 17.1°C than those of **M$_4$**.

3.2. *Mesomorphism and thermal properties of the polymers*

The mesomorphism of the polymers was investigated with POM and DSC. POM results showed that **P$_1$**−**P$_8$** exhibited typical nematic thread-like texture on heating and cooling cycles. As an example, the optical textures of **P$_1$** are shown in Fig. 2. Table 3 shows the phase transition temperatures of **P$_1$**−**P$_8$**. As seen from the data listed in table 3, the eight polymers all showed a melting transition, this indicated they were semi-crystalline polymers. Similar to the above monomers, chemical structures also affect the phase behavior of **P$_1$**−**P$_8$**. Moreover, the same tendency was seen. For example, T_m and T_i of **P$_2$** with six methylene spacer decreased by 24.5 and 17.9°C than those of **P$_1$** with two methylene spacer; T_m and T_i of **P$_3$** with four phenyl rings in the mesogenic core increased by 35.2 and 109.4°C than those of **P$_1$** with three phenyl rings; T_m and T_i of **P$_5$** with terminal pentyl group decreased by 5.3 and 5.9°C than those of **P$_1$** with terminal ethyl group. In addition, the mesophase temperature ranges of **P$_1$**−**P$_8$** were greater than those of the monomers. Such behavior could be attributed to the polymerization effect.

The thermal stability of the polymers **P$_1$**−**P$_8$** was detected with TGA. The corresponding thermal decomposition data are listed in Table 3. The temperatures at which 5 % weight loss occurred (T_d) of **P$_1$**−**P$_8$** were above 330°C, this indicated that they had high thermal stability under the nitrogen atmosphere.

Table 3. The phase transition temperatures and decomposition temperatures of polymers.

Polymer	T_g (°C)	T_m (°C)	T_i (°C)	T_d[b] (°C)
P_1	43.1	96.2	233.1	370
P_2	—	71.7	215.2	353
P_3	57.3	131.5	342.5[a]	348
P_4	—	109.8	333.6[a]	345
P_5	—	90.9	227.2	350
P_6	—	68.5	213.3	347
P_7	—	122.6	331.7[a]	339
P_8	—	99.3	324.8[a]	337

[a]Data obtained by POM;
[b]Temperature at which 5% weight loss occurred.

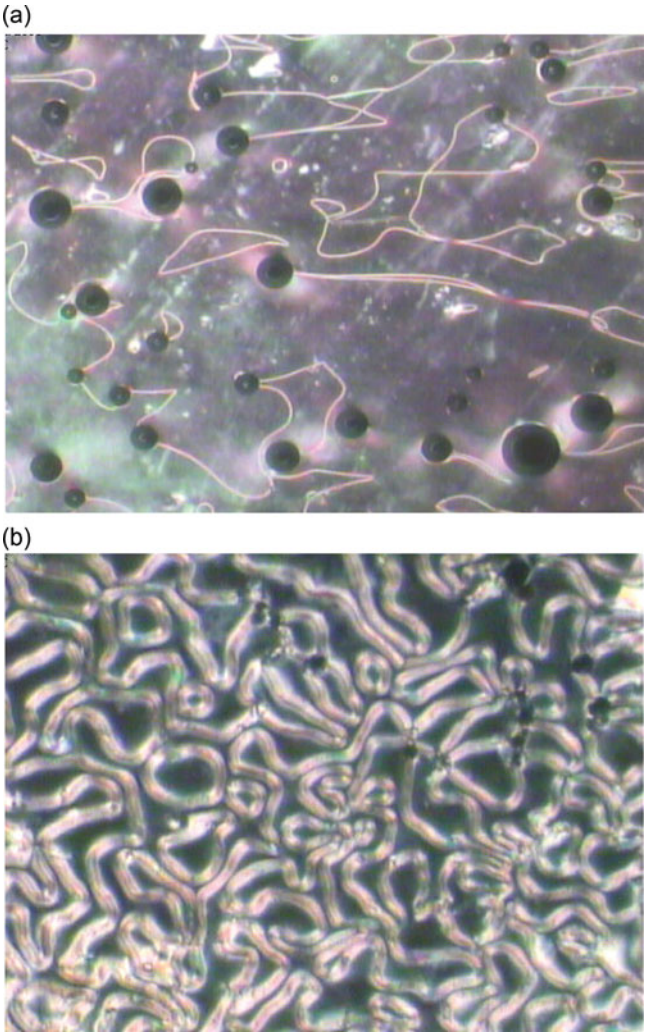

Figure 2. Optical textures of $\mathbf{P_1}$ (200×). (a) thread-like texture of nematic phase; (b) thread-like texture of nematic phase.

4. Conclusions

Eight new LC monomers and polymers were synthesized and characterized. $\mathbf{M_1}$−$\mathbf{M_8}$ all showed enantiotropic nematic thread-like texture and schlieren texture; $\mathbf{P_1}$−$\mathbf{P_8}$ all exhibited nematic thread-like texture. The experimental results demonstrated that the T_m and T_i of eight monomers and corresponding polymers all decreased with increasing the spacer length or flexibility of the terminal group, however, their T_m and T_i all increased with increasing the rigidity of the mesogenic core. The T_d of all the obtained polymers was greater than 335°C.

Acknowledgments

The authors are grateful to Science and Technology Committee of Liaoning Province (2013020103) and Science and Technology Bureau of Shenyang (F14-231-1-05) for financial support of this work.

References

[1] Lee, J. D., & Eringen, A. C. (1974). In *Liquid Crystals and Ordered Fluids*; Johnson, J. F., & Porter, R. S., (Eds.), Plenum: New York, NY.
[2] Trokhymchuk, A. (2010). *Condens. Matter. Phys.*, *13*, 370021.
[3] Lee, M., Choi, B. K., & Zin, W. C. (2001). *Chem. Rev.*, *101*, 3869.
[4] Tschierske, C. (2002). *Curr. Opin. Colloid In.*, *7*, 69.
[5] Pauluth, D., & Tarumi, K. J. (2004). *Mater. Chem.*, *14*, 1219.
[6] Goodby, J. W., Saez, I. M., Cowling, S. J., Görtz, V., Draper, M., Hall, A. W., Sia, S., Cosquer, G., Lee, S. E., & Raynes, E. P. (2008). *Angew. Chem.*, *47*, 2754.
[7] Keizer, S. H. M., & Sijbesma, R. P. (2005). *Chem. Soc. Rev.*, *34*, 226.
[8] Le Barney, P., Dubois, J. C., Friedrich, C., & Noel, C. (1986). *Polym. Bull.*, *15*, 341.
[9] Hsu, C. S., & Percec, V. J. (1989). *Polym. Sci. Polym. Chem. Ed.*, *27*, 453.
[10] Hsiech, C. J., Wu, S. H., Hsiue, G. H., & Hsu, C. S. (1994). *J. Polym. Sci. Part A: Polym. Chem.*, *32*, 1077.
[11] Wu, Y. H., Lu, Y. H., & Hsu, C. S. (1995). *J. Macromol. Sci.* A, *32*, 1471.
[12] Hu, J. S., Zhang, B. Y., Pan, W., & Zhou, A. J. (2005). *Liq. Cryst.*, *32*, 441.
[13] Liu, J. H., & Yang, P. C. (2006). *Polymer*, *47*, 4925.
[14] Hu, J. S., Li, D., Zhang, W. C., & Meng, Q. B. (2012). *J. Polym. Sci. Part A: Polym. Chem.*, *50*, 5049.
[15] Hu, J. S., Li, Q., Liu, Y. N., Song, Y. T., & Li, W. (2013). *Liq. Cryst.*, *40*, 1095.
[16] Brettar, J., Burgi, T., Donnio, B., Guillon, D., Klappert, R., Scharf, T., & Deschenaux, R. (2006). *Adv. Funct. Mater.*, *16*, 260.
[17] Hammond, M. R., & Mezzenga, R. (2008). *Soft Matter.*, *4*, 952.
[18] Liu, J. H., Wang, Y. K., Chen, C. C., Yang, P. C., Hsieh, F. M., & Chiu, Y. K. (2008). *Polymer 49*, 3938.
[19] Yang, S. H., & Hsu, C. S. (2009). *J. Polym. Sci. Part A: Polym. Chem.*, *47*, 2713.
[20] Serra, F., Matranga, M. A., Ji, Y., & Terentjev, E. M. (2010). *Opt. Express*, *18*, 575.
[21] Ohm, C., Haberkorn, N., Theato, P., & Zentel, R. (2011). *Small*, *7*, 194.
[22] Wang, A., Kawabata, K., & Goto, H. *Materials*, *6*, 2218.
[23] Portugall, M., Ringsdorf, H., & Zentel, R. (1982). *Makromol. Chem.*, *183*, 2311.
[24] Mihata, T., Nomura, K., Funaki, K., & Koide, N. (1997). *Polym. J.*, *29*, 303.
[25] Hu, J. S., Zhang, B. Y., Jia, Y. G., & Wang, Y. (2003). *Polym. J.*, *35*, 160.
[26] Dejeu, W. H. (1977). *Mol. Cryst. Liq. Cryst.*, *40*, 1.